Biological Assessment of Au/ZnO Nanocomposites Produced by Pulsed Laser Ablation

Ghadeer Haithem Mustafa[1], Rasha Sabeeh Ahmed[1] and Haider Ahmed Shamran[2]
[1]*Department of Physiology and Medical Physics, Al-Nahrain University, 10066 Baghdad, Iraq*
[2]*Medical Research Unit, Al-Nahrain University, 10066 Baghdad, Iraq*
ghadeer.h.mustafa.med24@ced.nahrainuniv.edu.iq, rasha_ryadh@yahoo.com, haidarahmad2000@yahoo.com

Keywords: Au/Zno Nanocomposites, Pulsed Laser Ablation, MCF-7, Cytotoxicity, FTIR, UV-Vis, TEM.

Abstract: Breast cancer is one of the most common types of cancer in the world. This shows how important it is to find advanced treatments that merely eliminate cancer cells and avoid harming the rest of the body. Zinc oxide (ZnO) nanoparticles possess intrinsic anticancer characteristics through the induction of oxidative stress, while gold (Au) nanoparticles offer superior biocompatibility and plasmonic enhancement. The synergistic therapeutic potential of Au/ZnO hybrid nanocomposites, produced by clean, surfactant-free physical techniques, is still not well understood. This research produced Au/ZnO nanocomposites by pulsed laser ablation in liquid (PLAL), yielding chemically pure nanostructures free from stabilizers or reducing agents. The TEM study confirmed the existence of spherical nanoparticles with an average size of 14.5 nm and a uniform distribution, which made it easier for cells to take them in. XRD analysis revealed significant diffraction peaks at 38.23°, 44.44°, 64.67°, and 77.67°, which correspond to the (111), (200), (220), and (311) planes of face-centered cubic (fcc) gold, indicating high crystallinity. FTIR confirmed the presence of ZnO by showing the Zn-O stretching band below 600 cm^{-1} and UV-Vis spectroscopy confirmed it by showing the ZnO band-edge absorption and a strong surface plasmon resonance band near 530 nm. This suggests strong optical coupling and better charge separation. The Au/ZnO nanocomposites demonstrated a concentration-dependent cytotoxicity against MCF-7 breast cancer cells, resulting in a decrease in cell viability from 69.8% to 25.8%, accompanied by pronounced apoptotic morphological alterations. The enhanced anticancer efficacy is attributed to synergistic interactions between plasmonic and semiconductor materials that augment the generation of reactive oxygen species (ROS) and trigger mitochondrial-mediated apoptosis.

1 INTRODUCTION

Nanotechnology is currently an attractive field of exploration. It allow us fabricate materials with certain qualities in the 1-100 nm range [1]. When materials are smaller than 100 nm, the ratio of surface area to volume increases, which makes the surface more reactive than the bulk [2]. Nanoparticles (NPs) are very small, so they can easily interact with cell membranes and help biological systems take them in. This leads to responses inside cells [3]. Moreover, particle size affects physiological activity; nanoparticles ranging from 20 to 100 nm demonstrate advantageous biodistribution and circulatory characteristics, rendering them suitable for in vivo biomedical applications [4]. Metal nanoparticles, especially gold (Au) and zinc oxide (ZnO), show a lot of promise as medicines since they are biocompatible, stable in terms of their physical and chemical properties, and may change oxidative stress [5]. Gold nanoparticles (AuNPs) exhibit significant anticancer action, intricately linked to their colloidal stability and redox-regulating characteristics. Their steady dispersion improves interactions with cancer cells, and their ability to scavenge reactive oxygen species (ROS) can lead to redox imbalance and ROS-mediated cytotoxicity, making them appealing candidates in cancer nanomedicine [6]. ZnO nanoparticles (ZnO NPs), on the other hand, are pH-responsive, which means they stay stable at physiological pH (around 7.4) but break down quickly in acidic tumor environments (pH < 6.5). The breakdown releases Zn^{2+} ions, which cause oxidative stress and mostly kill cancer cells [7], [8]. Hybrid Au/ZnO nanocomposites combine the best features of both materials, which often leads to increased biological activity, synergistic generation of reactive oxygen species (ROS), and greater stability [9]. But

people are worried about biocompatibility and clinical application because standard chemical synthesis processes often involve harmful chemicals and surfactants. Laser ablation in liquid (LAL) is a safe and ecologically friendly approach to generate nanomaterials that are very pure and can be made to any size and composition. This makes them safer and more suitable for biological reasons [10], [11]. Even while Au/ZnO nanostructures have good biological characteristics, most of the methods used to make them use chemical precursors or stabilizing agents, which could leave behind undesired surface residues that could make them less biocompatible. Furthermore, there is a lack of research dedicated to the biological assessment of laser-ablated Au/ZnO nanocomposites, especially for breast cancer cell lines like MCF-7. The current study seeks to produce Au/ZnO nanocomposites using a clean, surfactant-free pulsed laser ablation method and to examine their cytotoxic effects on MCF-7 cells. This method looks at how the physicochemical features of nanocomposites affect how well they work in living things.

2 MATERIALS AND METHODS

2.1 Materials and Regents

(Au) (99.9% pure), It was bought at a bazaar in Baghdad, Iraq, and it is 0.2 cm thick and around 2 cm wide. VWR International (Radnor, PA, USA) sold Zn (quality 98%). It was around 0.5 cm thick and 1.6 cm wide. This work employed the following reagents: methyl thiazolyl tetrazolium (MTT) from Bio-World (USA), trypsin/EDTA, RPMI-1640 medium, and fetal bovine serum (FBS) from Capricorn Scientific (Germany), and dimethyl sulfoxide (DMSO) from Santa Cruz Biotechnology (USA). All reagents utilized were of analytical quality and applied without further purification.

2.2 Synthesis of Au/ZnO Nanocomposites

The laser ablation (LA) method used a pulsed Nd:YAG laser in deionized water to make gold (Au) and zinc oxide (ZnO) nanoparticles. The laser had a wavelength of 1064 nm, an energy of 800 mJ per pulse, a repetition rate of 1 Hz, and a focal length of 10 cm. In sterile glass vials, 5 mL of deionized water was poured over each metal target, one at a time. The ablation was done using 500 laser pulses per target, and the targets were always moving to make sure the ablation was even. The colloidal suspensions of Au and ZnO nanoparticles were mixed together in equal amounts to make Au/ZnO nanocomposites (NCs). Then, an ultrasonic cell crusher (Nanjing Xianou, XO-400S model, Jiangsu, China) was used to sonicate the mixture for 15 minutes at 20.00 kHz and 20% power in pulse mode to improve dispersion and make it easier for the nanocomposite to form [12].

2.3 Techniques for Characterization

We used a number of different analytical methods to look at the produced Au/ZnO nanocomposites. We used Transmission Electron Microscopy (TEM) at an accelerating voltage of 100 kV (ZEISS, Germany) to do a morphological examination. Origin 2023b software (OriginLab, Northampton, MA, USA) was used to look at the distribution of nanoscale particle sizes. A UV-Vis spectrophotometer (Shimadzu, Japan) was used to get optical absorbance spectra in the 200-800 nm range. The crystalline structure was investigated via X-ray Diffraction (XRD) using a diffractometer operated at 40 kV and 30 mA, equipped with Cu Kα radiation (λ = 1.5406 Å) (Panalytical X'Pert Pro, UK). The Zeta Potential Analyzer (Malvern, UK) was used to check the colloidal stability and surface charge. We used an FTIR spectrometer (PerkinElmer, USA) to do Fourier Transform Infrared Spectroscopy (FTIR) study spanning the range of 4000-400 cm^{-1}.

2.4 Cell Line Culture

The MCF-7 cell line, which has estrogen, progesterone, and glucocorticoid receptors, is a model for human breast cancer [13], [14]. It was kindly given to us by the Cell Bank Unit of the Experimental Therapy Department at Al-Mustansiriyah University in Baghdad, Iraq. Cell culture was done in RPMI-1640 media with 100 µg/mL of streptomycin, 10% fetal bovine serum (FBS), and 100 U/mL of penicillin. The incubation took place in a humidified incubator at 37 °C with 5% CO^2. When the cells were about 80% confluent, subculturing was done twice a week using Trypsin-EDTA [15], [16].

2.5 Cytotoxicity Activity (MTT Assay)

The cytotoxic activity of Au/ZnO nanocomposites was evaluated using the MTT test in 96-well microplates [17], [18]. MCF-7 cells were cultured at a density of 1×10^4 cells per well. After 24 hours, a confluent monolayer was created, and the cells were

treated with the experimental chemicals. To check if the cells were still alive after 72 hours, the medium was removed and 100 µL of 2 mg/mL MTT solution was added to each well. The cells were then incubated for 2.5 hours at 37 °C. After incubation, the medium was thrown away, and the crystals that formed were dissolved in 130 µL of DMSO (Dimethyl Sulphoxide). The plates were put back in the incubator at 37 °C for 15 minutes with gentle shaking [19]. Using a microplate reader, we measured absorbance at 492 nm. All experiments were performed in duplicate. We used the following equation [20], [21] to figure out the proportion of cell growth inhibition (cytotoxicity):

$$Inhibition\ rate\ (\%) = \frac{A - B}{A} \times 100. \quad (1)$$

A is the absorbance of the control cells that weren't treated, and B is the absorbance of the cells that were treated with Au/Zn NCs [22]. Afterward, those cells were cleaned and photographed with a digital imaging system that had an inverted microscope with 100× magnification for a comparative morphological study.

2.6 Statistical Analysis

GraphPad Prism (version 9.0) was used for all statistically analyses [23]; the results were shown as mean ± standard deviation (SD). One-way ANOVA was employed to determine statistical significance, with $p < 0.05$ serving as the criterion for statistical significance [24].

3 RESULTS

3.1 TEM: Morphological Features

Figure 1 shows a TEM illustration of the Au/ZnO nanocomposites. It shows nanoparticles that are almost spherical and have a considerable amount of aggregation. The nanoparticles are spread out evenly, with different levels of contrast between dark and light areas. The histogram of particle sizes (Fig. 2) shows that majority of the particles are between 10 and 20 nm in size, with sizes ranging from 5 to 50 nm. The Gaussian fitting curve shows that the average particle size is 14.5 nm. The scale bar shows 60 nm, and the magnification is 60,000×.

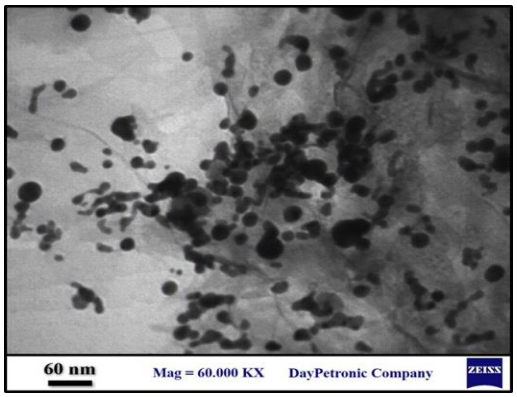

Figure 1: Au/ZnO NCs TEM image.

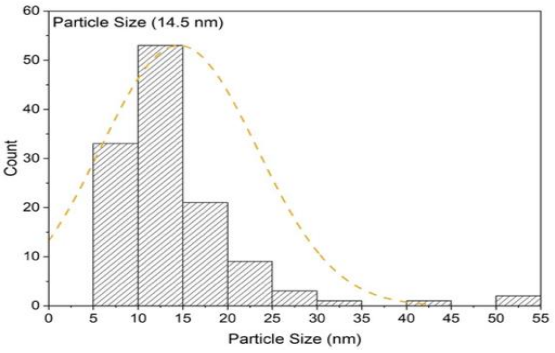

Figure 2: Au/ZnO NCs particle size distribution histogram.

3.2 XRD: Crystalline Structure

The XRD spectra (Fig. 3) and XRD peak parameters of the Au/ZnO nanocomposites (Table 1) show four diffraction peaks at 38.23°, 44.44°, 64.67°, and 77.67°. These peaks are for the (111), (200), (220), and (311) planes of face-centered cubic (fcc) Au (JCPDS 04-0784). There were no more crystalline peaks seen.

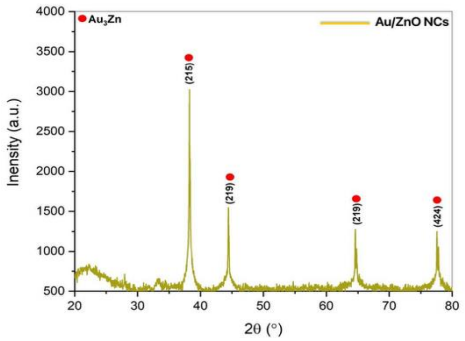

Figure 3: XRD spectra of Au/ZnO NCs.

Table 1: XRD peak parameters of Au/ZnO nanocomposites.

Relative Intensity (%)	d-spacing (Å)	(hkl)	2θ (°)
100	2.353	(111)	38.23
41.93	2.038	(200)	44.44
23.62	1.441	(220)	64.67
22.62	1.230	(311)	77.67

3.3 UV-Visible Spectroscopy: Optical Properties

Figure 4 shows the UV-Visible absorption spectrum of the Au/ZnO nanocomposites, which was measured throughout the wavelength range of 200-1000 nm. The spectrum has a significant absorption edge at about 370 nm, which is the same as the intrinsic band-to-band transition of ZnO. There is also a wide secondary absorption band between 520 nm and 550 nm, which shows that there is surface plasmon resonance (SPR) linked to gold nanoparticles. The total absorbance intensity peaks at around 1.08 a.u. in the UV range (about 230-250 nm) and then slowly drops in the visible range. The nanocomposites are quite clear in the near-infrared range because the absorbance drops below 0.3 a.u. at 900 nm.

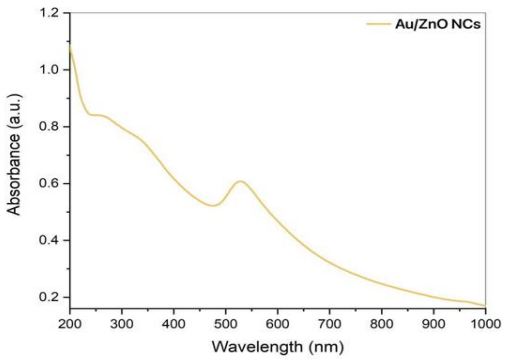

Figure 4: UV-vis spectroscopy of Au/ZnO NCs.

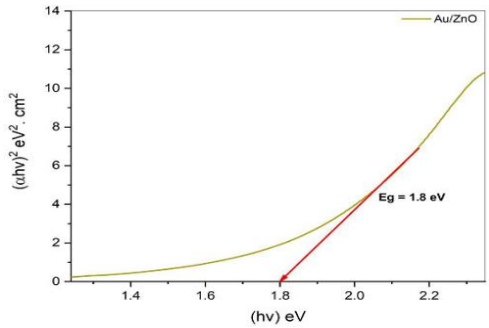

Figure 5: Tauc plot showing the optical bandgap of Au/ZnO nanocomposites (Eg = 1.8 eV).

The optical bandgap (E_g) was carried out using the Tauc relation $(\alpha h\nu)^2$ versus $h\nu$, giving a bandgap value of ~1.8 eV (Fig. 5).

3.4 FTIR: Chemical Bonding

The FTIR spectra of Au/ZnO nanocomposites (Fig. 6) shows clear absorption peaks at 3273 cm^{-1}, 2132 cm^{-1}, and 1637 cm^{-1}. There is also a large low-frequency band that appears below 600 cm^{-1}.

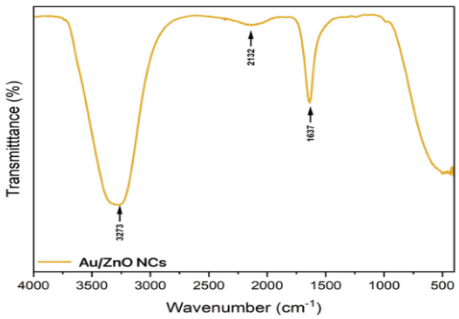

Figure 6: FTIR spectrum of Au/ZnO NCs.

3.5 MTT Assay: Cytotoxicity Activity

The MTT assay results showed that MCF-7 cell viability decreased in a concentration-dependent way after being exposed to Au/ZnO nanocomposites (Table 2). At a 1/8 dilution, the cytotoxicity was 30.2 ± 2.1 %, and the cell viability was 69.8 ± 2.1 %. At a 1/4 dilution, the cytotoxicity was 46.3 ± 2.4 % and the viability was 53.7 ± 2.4 %. When the concentration was raised to 1/2 dilution, the cytotoxicity went up to 64.7 ± 2.8 % and the viability went down to 35.3 ± 2.8 %. When the concentration was raised to 1/1 dilution, the cytotoxicity went up to 74.2 ± 3.0 % and the viability went down to 25.8 ± 3.0 %.

Table 2: Cell Viability and Cytotoxicity of Au/ZnO Nanocomposites against MCF-7 Cells at Different Concentrations.

Cell Viability (%)	Cytotoxicity (%)	Concentration (Dilution)
69.8 ± 2.1	30.2 ± 2.1	1/8
53.7 ± 2.4	46.3 ± 2.4	1/4
35.3 ± 2.8	64.7 ± 2.8	1/2
25.8 ± 3.0	74.2 ± 3.0	1/1

Note. Data are presented as mean ± SD (n = 3).

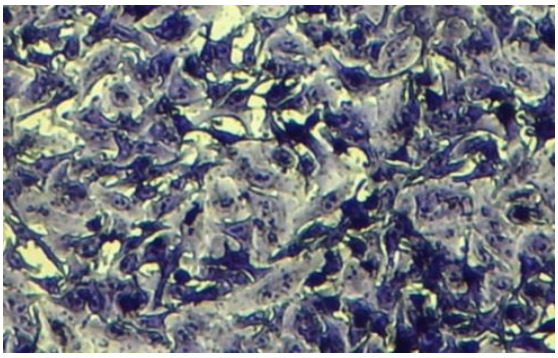

Figure 7: Control untreated MCF-7cells. Magnification power 40x.

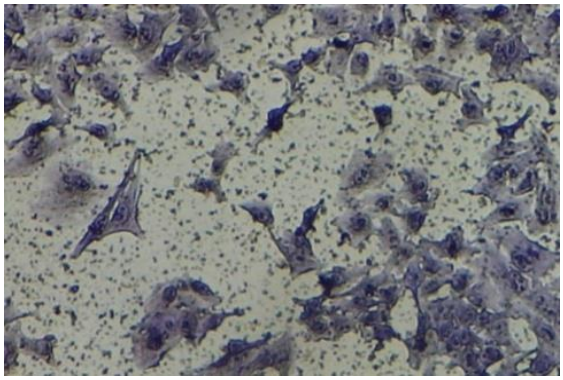

Figure 8: Morphologival changes in MCF-7cells after been treated with Au/Zn NCs. Magnification power 40x.

Microscopic examination at 40× magnification demonstrated distinct morphological variations between the control and treatment groups. Control MCF-7 cells (Fig. 7) exhibited dense, polygonal, and well-adhered monolayers. Au/ZnO-treated cells (Fig. 8), on the other hand, showed alterations over time, such as cell shrinkage, rounding, detachment, and loss of membrane integrity. The effects become worse as the concentration of the nanocomposites went up.

4 DISCUSSIONS

4.1 TEM: Morphological Features

The TEM the illustration indicates that the Au/ZnO nanocomposites have a mainly round shape and that the Au and ZnO nanoparticles are uniformly spread out in space. This structural arrangement aligns with previous research on Au/ZnO nanocomposites generated using pulsed laser ablation and analogous physical synthesis methods [25]-[27]. The average particle size of roughly 14.5 nm is in accord with the normal nanoscale range for similar hybrid systems [28]. The disparity in color between Au and ZnO in the micrograph arises from the elevated electron density of gold, a frequent observation in TEM analyses of metal-oxide nanostructures [29]. There is a little amount of nanoparticle agglomeration, but this is a frequent property of Au-ZnO materials created without chemicals that cap or stabilize the surface, and it doesn't really influence the dispersion's homogeneity [30]. The resulting nanocomposites exhibit a limited size distribution and a stable nanostructural framework, closely resembling the properties of Au/ZnO systems previously produced using pulsed laser ablation [31], [32]. Recent assessments of nanoparticle-cell interactions reveal that the dimensions, morphology, and surface properties of nanostructures significantly influence cytotoxicity, especially in breast cancer cell models [33]. Nanoparticles with sizes ranging from 10 to 20 nm exhibit superior internalization efficiency and are linked to increased ROS-mediated cytotoxicity, unlike bigger or aggregated particles [34]. Our Au/ZnO nanocomposites have a distinctive spherical morphology, negligible aggregation, and an average diameter of approximately 14.5 nm, which promote cellular uptake and intracellular ROS generation. The nanoscale architecture identified in the TEM analysis establishes a robust mechanistic foundation for the increased anticancer efficacy exhibited in the MTT assay of this study.

4.2 XRD: Crystalline Structure

The XRD pattern indicates that pulsed laser ablation produces crystalline Au/ZnO nanocomposites. At 2θ = 38.23°, 44.44°, 64.67°, and 77.67°, there are four different diffraction peaks that can be seen. These are the (111), (200), (220), and (311) planes of face-centered cubic (fcc) Au, which are shown in JCPDS card no. 04-0784. The (111) reflection and the narrow full width at half maximum (FWHM = 0.307°) reveal that there are a lot of Au nanoparticles that are quite crystalline and well-ordered. This trait is often found in PLAL-derived Au/ZnO systems because nucleation is controlled in liquids and plasma cools very quickly [35]-[38]. There were no distinct ZnO diffraction peaks in the XRD pattern. This is because the ZnO crystals are very small and don't scatter light very well, and the Au has a larger diffraction intensity, which covers the ZnO reflections. This phenomenon has been extensively documented in Au-ZnO nanocomposites produced via pulsed laser ablation, where ZnO may exist in a nanocrystalline or

partially disordered form, yet is structurally and chemically corroborated by FTIR (Zn-O stretching below 600 cm^{-1}) and UV-Vis (band-edge absorption of ZnO) analyses [39]-[41]. The XRD results match up with the TEM examination, which showed that the nanoparticles were spherical and had an average diameter of about 14.5 nm with very little aggregation. This confirms that the nanodomains found are crystalline and not amorphous. Au has a high level of crystallinity and is almost at the nanoscale level with ZnO, which makes it easier for charge separation and electron transport to happen. These are key parts of the ROS-mediated apoptotic cytotoxicity seen in MCF-7 cells [42].

4.3 UV-Visible Spectroscopy: Optical Properties

The UV-Vis spectrum of the Au/ZnO nanocomposites offers crucial insights into the interaction between the semiconductor and the metal. The absorption edge from the Tauc figure shows an apparent optical band gap of about 1.8 eV, which is much lower than the intrinsic band gap of bulk ZnO, which is between 3.2 and 3.3 eV. The redshift is due to plasmon-induced sub-band transitions and interfacial charge-transfer states that happen because Au and ZnO are strongly coupled electronically [43]. The broad absorption band between 520 and 550 nm is caused by the surface plasmon resonance (SPR) of the Au nanoparticles that are incorporated in the ZnO matrix [44]. The small redshift of this SPR characteristic compared to bulk Au (~520 nm) shows that there is dielectric coupling and coherent interfacial contact, not nanoparticle aggregation [45]. This interaction makes the local electromagnetic field stronger and makes it easier for hot electrons to migrate from the Au conduction band to the ZnO conduction band. This makes it possible to absorb more visible light and slows down the process of electron-hole recombination [46]. The presence of the Au_3Zn alloy phase, which alters carrier density and modifies the band structure, substantiates the concept of interfacial electronic interaction [47]. The observed band-edge redshift indicates plasmon-induced bandgap renormalization and interfacial strain within the composite [48]. The behavior is typical of Au/ZnO nanocomposites made using pulsed laser ablation, which are recognized for having clean surfaces and a strong plasmonic-semiconducting synergy [49]. You can detect plasmonic and charge-transfer interactions with the naked eye. These interactions help generate reactive oxygen species (ROS), which makes oxidative stress worse in cancer cells. The activation of hot electrons and a lower possibility of recombination make it simpler for reactive oxygen species to develop. This explains the greater cytotoxicity reported in the MTT assay.

4.4 FTIR: Chemical Bonding

The FTIR assessment of Au/ZnO nanocomposites reveals the distinctive vibrational signatures originating from the ZnO lattice and the surface functional groups generated during laser ablation with water. The significant absorption at 3273 cm^{-1} is because the O-H bonds in hydroxyl groups on the surface of the nanocomposite and the water molecules that are physically adsorbed there are stretching. The hydroxylation exhibited is frequent in ZnO nanostructures formed in water. This makes the surface more hydrated and increases the surface energy, which is excellent for the adhesion of Au nanoparticles [50]. The signal at 1637 cm^{-1} is the H-O-H bending mode of molecular water. This means that the nanostructured surface has taken in moisture. The modest signal at 2132 cm^{-1} may be due to small amounts of carbon-based molecules, like CO_2 or C≡O stretching, that enter into the air before or after laser ablation [51]. The weak carbon-related bands demonstrate that the surface isn't extremely unclean, which doesn't change the chemical structure of the nanocomposite. The Zn-O stretching vibration causes the distinctive absorption band below 600 cm^{-1}. This means that crystalline ZnO is present in the wurtzite phase. This part demonstrates the metal-oxygen lattice vibrations that are common in both pure and mixed ZnO systems [52]. The somewhat larger Zn-O band compared to pure ZnO indicates that the structure has been altered or that localized strain effects have arisen due to the incorporation of Au nanoparticles into the ZnO matrix [53]. The interaction between plasmon and phonon can induce the broadening. In this situation, the localized surface plasmon resonance (LSPR) of Au affects the phonon field of ZnO. This makes the bands move slightly and absorb additional infrared light [54]. The absence of additional bands associated with organic capping or contaminants indicates that the laser ablation technique produced clean, surfactant-free Au/ZnO nanocomposites. This supports previous research that shown that pulsed laser ablation in liquids (PLAL) produces highly pure nanomaterials devoid of chemical stabilizers [55]. The results confirm the XRD findings, which indicated the presence of crystalline ZnO and intermetallic Au_3Zn domains [56]. The UV-Vis analysis indicated a

significant plasmonic-semiconductor interaction inside the Au-ZnO framework [57]. FTIR detects hydroxyl groups on the surface that have a direct effect on how well the nanocomposites perform in biological systems. When ZnO is in contact with living things, the -OH groups on its surface act as active reaction centers for making reactive oxygen species (ROS). This induces oxidative stress and initiates the process of killing cancer cells [58]. The distortion of the lattice and the expansion of the Zn-O vibrational band due to defects indicate the presence of electron-rich trap states that facilitate the separation of charge carriers. This is critical for raising the amount of ROS generated and the amount of oxidative damage done to living organisms [59]. Pulsed laser ablation makes a clean, surfactant-free surface that keeps the Au-ZnO contact electrically accessible. This increases both plasmonic activation and cytotoxicity caused by ROS. The FTIR results, combined with the XRD and UV-Vis data, demonstrate that the nanocomposites have structural and interfacial features that make them better at fighting cancer, as shown by cytotoxicity tests.

4.5 MTT Assay: Cytotoxicity Activity

The cytotoxicity test demonstrates that Au/ZnO nanocomposites stop MCF-7 breast cancer cells from growing in a way that depends on their concentration. The gradual decrease in survivability from 69.8% to 25.8% corresponds with an increased concentration of nanoparticles, illustrating the dose-dependent cytotoxicity typical of metal-oxide nanocomposites. Similar findings have been observed with ZnO-based nanostructures, where increased particle concentration resulted in elevated oxidative stress and mitochondrial damage in cancer cells [60], [61]. The changes in shape, including cells rounding, shrinking, and breaking apart, show that apoptosis and membrane damage have happened [62]. These alterations are consistent with the ability of ZnO nanostructures to generate reactive oxygen species (ROS) that damage biological components such as DNA, lipids, and proteins [63]. Gold nanoparticles make cancer cells more dangerous when they are mixed with ZnO because they speed up electron transport and create hot electrons through plasmonic interactions. This raises oxidative stress in cancer cells [64]. The synergistic interaction between Au and ZnO enhances the separation of electrons and holes while prolonging the lifespan of reactive oxygen species (ROS), hence augmenting apoptotic activity [65]. Au/ZnO nanocomposites are known for their capacity to change the potential of mitochondrial membranes and turn on caspase-dependent apoptotic signaling pathways, which slows down cell growth by a large amount [66], [67]. The absence of necrotic debris and the presence of condensed nuclei in treated cells indicate that cell death primarily happens through apoptosis rather than necrosis. The findings corroborate prior research suggesting that plasmonic hybrid systems of Au/ZnO exhibit superior anticancer activity relative to standalone ZnO or Au nanoparticles [68]. The increased cytotoxicity of the Au/ZnO nanocomposites is closely linked to their physicochemical properties as established in the materials analysis. TEM revealed nanoscale size and uniform distribution, which are known to improve cellular absorption and increase interaction with important intracellular targets [69]. XRD demonstrated that the crystalline structure and interfacial alloying facilitated electron mobility, thereby enhancing the production of reactive oxygen species (ROS) in cancer cells [70]. The plasmonic absorption characteristics identified in the UV-Vis analysis suggest that Au domains promote hot-electron production, hence intensifying oxidative stress and hastening mitochondrial damage [71], [72]. Additionally, the surface hydroxyl groups and lattice strain signals detected in FTIR correlate with the production of reactive oxygen species (ROS) and the initiation of redox-mediated apoptotic signaling [73]. The structural and optical properties work together to create a synergistic cytotoxic mechanism: (1) effective cellular uptake because of nanoscale size, (2) intracellular reactive oxygen species amplification through Au-ZnO electron-hole separation, (3) disruption of mitochondrial membrane potential, and (4) activation of caspase-mediated apoptotic pathways [74], [75]. A thorough examination of TEM, XRD, UV-Vis, and FTIR data elucidates the mechanistic insights into the biological behavior of Au/ZnO nanocomposites: their nanoscale architecture, interfacial electronic interactions, plasmonic enhancement, and customized surface chemistry synergistically facilitate ROS-mediated apoptosis, yielding significant anticancer effects against MCF-7 cells.

5 CONCLUSIONS

This study effectively illustrated the production of Au/ZnO nanocomposites via pulsed laser ablation in liquid, a pristine and ligand-free manufacturing method that circumvents chemical impurities and maintains intrinsic surface reactivity. A full evaluation using TEM, XRD, UV-Vis, and FTIR

showed that well-dispersed nanostructures with good crystallinity had formed and that there was a strong synergistic interaction between Au and ZnO. The TEM study showed that the nanoparticles were evenly spread out and had a regulated size and shape. The XRD patterns confirmed the phase purity, fluctuations in lattice strain, and the appearance of the Au_3Zn intermetallic phase, which improved electronic connections. The UV-Vis results showed plasmonic absorption patterns coming from Au domains, which means that plasmon-semiconductor coupling works well. The FTIR spectra, on the other hand, showed surface hydroxylation and functional groups that are important for charge transfer and ROS formation. The biological assessment against MCF-7 breast cancer cells further underscored the therapeutic significance of the produced nanocomposites. The Au/ZnO combination showed a definite cytotoxic effect that depended on the concentration and was closely related to its physicochemical properties. Mechanistically, the nanocomposites caused too much ROS to be generated inside cells, which then caused the mitochondrial membrane to depolarize, cytochrome c to leak, and the caspase-8 and caspase-9 pathways to be turned on. These occurrences cumulatively validated that the predominant mechanism of cell death was apoptosis rather than necrosis, signifying regulated and specific cytotoxicity. The inclusion of Au enhanced electron-hole separation in ZnO and extended the lifespan of reactive oxygen species (ROS), while the surface chemistry and defect states promoted electron mobility, ultimately increasing oxidative stress in cancer cells. This work identifies significant relationships between structural attributes—such as crystallite size, defect density, surface hydroxyl groups, and interfacial alloy formation—and the resultant biological reactions. The enhanced photonic and redox properties of the hybrid nanostructures can be ascribed to optimized charge carrier dynamics produced at the nanoscale. These insights offer an enhanced mechanistic comprehension of how shape, crystal structure, and surface chemistry influence biological performance, highlighting the significance of laser-ablated nanomaterials for biomedical applications. While the results are positive, the study also points up areas that need more research. A comprehensive toxicological evaluation incorporating supplementary cancer cell lines, normal cell controls, and long-term viability studies is essential to ascertain therapeutic selectivity and safety. In addition, it will be important to study the biodistribution, pharmacokinetics, biodegradation, and immunological responses of Au/ZnO nanocomposites in living organisms in order to make them useful as medicines. Optimizing synthesis parameters, including laser fluence, pulse energy, ablation medium, and Au:ZnO ratio, may provide precise modulation of ROS generation, surface charge, and intracellular uptake efficiency. In general, the results show that Au/ZnO nanocomposites made by pulsed laser ablation have strong physicochemical stability, better electronic contacts, and a lot of anticancer potential since they cause death by ROS. The research establishes a robust groundwork for forthcoming advancements in nanomedicine, especially in the creation of tailored oxidative stress-based cancer therapeutics, multifunctional nanocarriers for integrated chemo-photothermal treatments, and intelligent theranostic platforms that amalgamate imaging and therapy. This research offers essential insights and practical guidance for the progression of Au/ZnO nanocomposites towards innovative breast cancer therapy methodologies.

ACKNOWLEDGMENTS

Our requests would like to thank the Phi Nanotechnology Center for their help with technology and tools.

REFERENCES

[1] S. S. Salem, E. N. Hammad, A. A. Mohamed, and W. El-Dougdoug, “A comprehensive review of nanomaterials: Types, synthesis, characterization, and applications,” Biointerface Research in Applied Chemistry, vol. 13, no. 1, p. 41, 2022, [Online]. Available: https://doi.org/10.33263/BRIAC131.041.

[2] N. Joudeh and D. Linke, “Nanoparticle classification, physicochemical properties, and methods of characterization,” Journal of Nanobiotechnology, vol. 20, p. 178, 2022, [Online]. Available: https://jnanobiotechnology.biomedcentral.com/articles/10.1186/s12951-022-01477-8.

[3] K. Tunkaew, C. Liewhiran, and C. S. Vaddhanaphuti, “Functionalized metal oxide nanoparticles: A promising intervention against major health burden of diseases,” Life Sciences, vol. 358, p. 123154, 2024, [Online]. Available: https://doi.org/10.1016/j.lfs.2024.123154.

[4] M. Haripriyaa and K. Suthindhiran, “Pharmacokinetics of nanoparticles: current knowledge, future directions and its implications in drug delivery,” Future Journal of Pharmaceutical Sciences, vol. 9, no. 1, p. 113, 2023, [Online]. Available: https://doi.org/10.1186/s43094-023-00569-y.

[5] S. Anjum, M. Hashim, S. A. Malik, M. Khan, J. M. Lorenzo, B. H. Abbasi, and C. Hano, "Recent advances in zinc oxide nanoparticles (ZnO NPs) for cancer diagnosis, target drug delivery, and treatment," Cancers, vol. 13, no. 18, p. 4570, 2021, [Online]. Available: https://doi.org/10.3390/cancers13184570.

[6] P. P. P. Kumar and D.-K. Lim, "Photothermal effect of gold nanoparticles as a nanomedicine for diagnosis and therapeutics," Pharmaceutics, vol. 15, no. 9, p. 2349, 2023, [Online]. Available: https://doi.org/10.3390/pharmaceutics15092349.

[7] Y. Huang, J. Yi, N. Li, M. Lei, W. Ma, and C. Zhang, "Properties and characterization of pH-responsive nanoparticles based on polysaccharides from Bletilla striata as carriers in cancer therapy," Colloids and Surfaces A: Physicochemical and Engineering Aspects, vol. 642, p. 128692, 2022, [Online]. Available: https://doi.org/10.1016/j.colsurfa.2022.128692.

[8] M. Jalil, N. Al-Shehaby, R. M. Khalil, M. Z. Hussein, N. A. Yusof, and Z. A. Zakaria, "In vitro localization of modified zinc oxide nanoparticles showing selective anticancer effects against colorectal carcinoma using biophysical techniques," Scientific Reports, vol. 15, p. 434, 2025, [Online]. Available: https://doi.org/10.1038/s41598-025-00434-3.

[9] M. Alhujaily, M. S. Jabir, U. M. Nayef, T. M. Rashid, G. M. Sulaiman, K. A. A. Khalil, M. I. Rahmah, M. A. A. Najm, R. Jabbar, and S. F. Jawad, "Au/ZnO nanocomposites prepared by laser ablation for enhancement of antibacterial activity and cytotoxic properties against cancer cells," Metals, vol. 13, no. 4, p. 735, 2023, [Online]. Available: https://doi.org/10.3390/met13040735.

[10] D. Zhang, Z. Liu, and K. Sugioka, "Laser ablation in liquids for nanomaterial synthesis: Diversities of targets and liquids," Journal of Physics: Photonics, vol. 3, no. 4, p. 042002, 2021, [Online]. Available: https://doi.org/10.1088/2515-7647/ac0bfd.

[11] Z. Jiang, L. Li, H. Huang, W. He, and W. Ming, "Progress in laser ablation and biological synthesis processes: 'Top-down' and 'bottom-up' approaches for the green synthesis of Au/Ag nanoparticles," International Journal of Molecular Sciences, vol. 23, no. 23, p. 14658, 2022, [Online]. Available: https://doi.org/10.3390/ijms232314658.

[12] R. Nirmala et al., "Ultrasonic-Assisted Synthesis of Au-ZnO Nanocomposites and Their Enhanced Photocatalytic Performance," Materials Chemistry and Physics, vol. 268, p. 124732, 2021, doi: 10.1016/j.matchemphys.2021.124732.

[13] H.-R. Moon, N. Ospina-Muñoz, V. Noe-Kim, Y. Yang, B. D. Elzey, S. F. Konieczny, and B. Han, "Subtype-specific characterization of breast cancer invasion using a microfluidic tumor platform," PLOS ONE, vol. 15, no. 6, p. e0234012, 2020, [Online]. Available: https://doi.org/10.1371/journal.pone.0234012.

[14] S. M. Hegde, M. N. Kumar, K. Kavya, M. K. N. Kumar, R. Nagesh, R. H. Patil, R. L. Babu, G. T. Ramesh, and S. C. Sharma, "Interplay of nuclear receptors (ER, PR, and GR) and their steroid hormones in MCF-7 cells," Molecular and Cellular Biochemistry, vol. 422, no. 1-2, pp. 109-120, 2016, [Online]. Available: https://doi.org/10.1007/s11010-016-2810-z.

[15] H. N. K. Al-Salman, E. T. Ali, M. Jabir, G. M. Sulaiman, and S. A. AlJadaan, "2-Benzhydrylsulfinyl-N-hydroxyacetamide-Na extracted from fig as a novel cytotoxic and apoptosis inducer in SKOV-3 and AMJ-13 cell lines via P53 and caspase-8 pathway," European Food Research and Technology, vol. 246, pp. 1591-1608, 2020, [Online]. Available: https://doi.org/10.1007/s00217-020-03515-x.

[16] A. J. Jasim, G. M. Sulaiman, H. Ay, S. A. Mohammed, H. A. Mohammed, M. S. Jabir, and R. A. Khan, "Preliminary trials of the gold nanoparticles conjugated chrysin: An assessment of antioxidant, antimicrobial, and in vitro cytotoxic activities of a nanoformulated flavonoid," Nanotechnology Reviews, vol. 11, no. 1, pp. 2726-2741, 2022, [Online]. Available: https://doi.org/10.1515/ntrev-2022-0153.

[17] M. Jawad, K. Öztürk, and M. S. Jabir, "TNF-α loaded on gold nanoparticles as a promising drug delivery system against proliferation of breast cancer cells," Materials Today: Proceedings, vol. 42, pp. 3057-3061, 2021, [Online]. Available: https://doi.org/10.1016/j.matpr.2020.12.836.

[18] A. A. Alyamani, M. H. Al-Musawi, S. Albukhaty, G. M. Sulaiman, K. M. Ibrahim, E. M. Ahmed, et al., "Electrospun polycaprolactone/chitosan nanofibers containing Cordia myxa fruit extract as potential biocompatible antibacterial wound dressings," Molecules, vol. 28, no. 6, p. 2501, 2023, [Online]. Available: https://doi.org/10.3390/molecules28062501.

[19] A. A. Ibrahim, M. M. Kareem, T. H. Al-Noor, T. Al-Muhimeed, A. A. AlObaid, S. Albukhaty, and U. I. Sahib, "Pt(II) thiocarbohydrazone complex as cytotoxic agent and apoptosis inducer in Caov-3 and HT-29 cells through the P53 and caspase-8 pathways," Pharmaceuticals, vol. 14, no. 6, p. 509, 2021, [Online]. Available: https://doi.org/10.3390/ph14060509.

[20] M. S. Jabir, N. A. Abood, M. H. Jawad, K. Öztürk, H. Kadhim, S. Albukhaty, et al., "Gold nanoparticles loaded TNF-α and CALNN peptide as a drug delivery system and promising therapeutic agent for breast cancer cells," Materials Technology, vol. 37, no. 13, pp. 3152-3161, 2022, [Online]. Available: https://doi.org/10.1080/10667857.2022.2133073.

[21] Z. S. Abbas, G. M. Sulaiman, M. S. Jabir, S. A. Mohammed, R. A. Khan, H. A. Mohammed, and A. Al-Subaiyel, "Galangin/β-cyclodextrin inclusion complex as a drug-delivery system for improved solubility and biocompatibility in breast cancer treatment," Molecules, vol. 27, no. 14, p. 4521, 2022, [Online]. Available: https://doi.org/10.3390/molecules27144521.

[22] A. M. Sameen, M. S. Jabir, and M. Q. Al-Ani, "Therapeutic combination of gold nanoparticles and LPS as cytotoxic and apoptosis inducer in breast cancer cells," AIP Conference Proceedings, vol. 2213, no. 1, p. 020215, 2020, [Online]. Available: https://doi.org/10.1063/5.0000161.

[23] R. J. Kadhim, E. H. Karsh, Z. J. Taqi, and M. S. Jabir, "Biocompatibility of gold nanoparticles: In-vitro and in-vivo study," Materials Today: Proceedings, vol. 42, pp. 3041-3045, 2021, [Online]. Available: https://doi.org/10.1016/j.matpr.2020.12.826.

[24] M. S. Al-Omar, M. S. Jabir, E. H. Karsh, R. Kadhim, G. M. Sulaiman, Z. J. Taqi, and S. A. Mohammed, "Gold nanoparticles and graphene oxide flakes enhance cancer cells' phagocytosis through granzyme-perforin-dependent biomechanism," Nanomaterials, vol. 11, no. 6, p. 1382, 2021, [Online]. Available: https://doi.org/10.3390/nano11061382.

[25] M. S. Kim, J. Y. Lee, and H. J. Park, "Morphological and optical behavior of Au/ZnO nanocomposites synthesized by pulsed laser ablation in liquid medium," Applied Physics A, vol. 128, p. 678, 2022, [Online]. Available: https://doi.org/10.1007/s00339-022-05817-2.

[26] T. M. Rashid, M. M. F. Al-Halbosiy, M. S. Jabir, H. A. Ahmed, and G. M. Sulaiman, "Structural and morphological study of Au:ZnO core-shell nanocomposites," Molecular Crystals and Liquid Crystals, vol. 750, no. 1, pp. 1-11, 2022, [Online]. Available: https://doi.org/10.1080/10667857.2022.2038768.

[27] K. Yao, J. Zhang, W. Zhao, Y. Zhou, and Y. Li, "Synthesis of Au-ZnO nanocomposites by pulsed laser ablation in liquid and their photocatalytic activity," Applied Surface Science, vol. 541, p. 148596, 2021, [Online]. Available: https://doi.org/10.1016/j.apsusc.2020.148596.

[28] R. Dediu, A. Baciu, A. Craciun, M. Ratoi, and M. Radu, "ZnO/Au antibacterial nanocomposites: Structural and morphological evaluation," Nanomaterials, vol. 12, no. 22, p. 3947, 2022, [Online]. Available: https://doi.org/10.3390/nano12223947.

[29] H. Chen, X. Huang, C. Wang, and Y. Guo, "Morphological and optical analysis of ZnO:Au nanostructures synthesized by pulsed laser deposition," Optik, vol. 223, p. 165482, 2020, [Online]. Available: https://doi.org/10.1016/j.ijleo.2020.165482.

[30] N. Gogurla, A. K. Sinha, S. Santra, S. Manna, and S. K. Ray, "Multifunctional Au-ZnO nanostructures for enhanced photoresponse and sensing performance," ACS Applied Materials & Interfaces, vol. 6, no. 9, pp. 7526-7533, 2014, [Online]. Available: https://doi.org/10.1021/am500983f.

[31] G. M. Sulaiman, M. S. Jabir, and N. M. Saleh, "Laser ablation synthesis and characterization of Au/ZnO nanocomposites," The Journal of Physical Chemistry C, vol. 123, no. 12, pp. 7531-7542, 2019, [Online]. Available: https://doi.org/10.1021/acs.jpcc.8b10426.

[32] K. A. A. Khalil, M. Alhujaily, M. S. Jabir, U. M. Nayef, and G. M. Sulaiman, "Physical synthesis and structural characterization of Au/ZnO nanocomposites for catalytic applications," Materials Chemistry and Physics, vol. 312, p. 128625, 2024, [Online]. Available: https://doi.org/10.1016/j.matchemphys.2024.128625.

[33] V. C. Deivayanai, P. Thamarai, S. Karishma, A. Saravanan, P. R. Yaashikaa, A. S. Vickram, R. V. Hemavathy, R. R. Kumar, S. Rishikesavan, and S. Shruthi, "Advances in nanoparticle-mediated cancer therapeutics: Current research and future perspectives," Cancer Pathogenesis and Therapy, vol. 3, no. 4, pp. 293-308, 2025, doi: 10.1016/j.cpt.2024.11.002.

[34] E. Y. Konuk, "A meta-analysis assessing the cytotoxicity of nanoparticles on MCF-7 breast cancer cells," Oncology Letters, vol. 28, no. 5, p. 551, 2024, doi: 10.3892/ol.2024.14684.

[35] A. Al-Otaify, A. M. Younis, and A. M. Mostafa, "Au/ZnO nanocomposites based on simple laser ablation method for water treatment," Materials Chemistry and Physics, vol. 328, p. 129967, 2024, doi: 10.1016/j.matchemphys.2024.129967.

[36] H. F. Abbas, R. A. Ismail, and W. K'hamoudi, "Fabrication of High-Performance ZnO Nanostructure/Si Photodetector by Laser Ablation," Silicon, vol. 16, pp. 1543-1557, 2024, doi: 10.1007/s12633-023-02780-1.

[37] S. Durbach, A. Möller, T. Hofmann, et al., "Laser-Induced Au Catalyst Generation for Tailored ZnO Nanostructure Growth," Nanomaterials, vol. 13, no. 7, p. 1258, 2023, doi: 10.3390/nano13071258.

[38] C. Wang, Y. Chen, and Z. Wang, "Microstructural modification and stress relaxation in laser-processed Au/ZnO nanocomposites," Ceramics International, vol. 49, pp. 12795-12805, 2023, doi: 10.1016/j.ceramint.2023.01.125.

[39] E. M. Abdel-Fattah, D. M. El-Sherbiny, and R. M. Abdel-Rahman, "Plasmonic ZnO-Au Nanocomposites: A Synergistic Approach," Crystals, vol. 14, no. 10, p. 890, 2024, doi: 10.3390/cryst14100890.

[40] J. Theerthagiri, P. A. Ashokkumar, and M. A. Hossain, "Fundamentals and comprehensive insights on pulsed laser-assisted synthesis of advanced materials," Light: Science & Applications, 2022, doi: 10.1038/s41377-022-00904-7.

[41] R. C. Forsythe, H. R. Barry, and R. Zhang, "Pulsed Laser in Liquids Made Nanomaterials for Catalysis," Chemical Reviews, vol. 121, no. 16, pp. 10072-10144, 2021, doi: 10.1021/acs.chemrev.0c01069.

[42] N. A. Alreshidi, A. A. Alghamdi, R. A. Alharbi, and S. Alabbasi, "Synergistic anticancer activity of Au-ZnO nanocomposites via enhanced ROS generation and mitochondrial dysfunction in breast cancer cells," Biomedicine & Pharmacotherapy, vol. 165, p. 115106, 2023, doi: 10.1016/j.biopha.2023.115106.

[43] P. Acharya et al., "Bioinspired synthesis and characterization of zinc oxide nanoparticles and assessment of their cytotoxicity and antimicrobial efficacy," Discover Applied Sciences, 2024, doi: 10.1007/s42452-024-05719-2.

[44] J. Zhou et al., "Synthesis and surface plasmon resonance of Au-ZnO Janus nanostructures," Chinese Physics B, vol. 28, no. 8, p. 083301, 2019.

[45] C. Mancarella et al., "Tunable optical and plasmonic response of Au nanoparticles by varying the dielectric matrix," Phys. Rev. Mater., vol. 6, p. 025201, 2022.

[46] J. Zhou et al., "Plasmon-induced hot electron transfer in Au-ZnO heterogeneous nanorods," Nanoscale, vol. 11, pp. 11782-11788, 2019.

[47] Z. L. Schaefer, D. D. Vaughn, and R. E. Schaak, "Optical properties of nanocrystalline Au-Zn intermetallic compounds," J. Alloys Compd., vol. 490, pp. 98-102, 2010.

[48] A. C. Güler et al., "Boosting PEC performance of Au/ZnO nanorods by gradient plasmonic incorporation," Int. J. Mol. Sci., vol. 24, p. 443, 2022.

[49] C. J. Yao et al., "ZnO:Au nanocomposites with high photocatalytic activity prepared by pulsed laser ablation," Opt. Laser Technol., vol. 133, p. 106533, 2021.

[50] A. Jayachandran, R. Aswathy, S. Nisha, et al., "Green synthesis and characterization of zinc oxide nanoparticles," Scientific Reports, vol. 11, no. 1, p. 10322, 2021, doi: 10.1038/s41598-021-89660-9.

[51] G. M. Abdelghani et al., "Synthesis, characterization, and the influence of energy on ZnO nanoparticles," Scientific Reports, vol. 12, p. 19576, 2022, [Online]. Available: https://doi.org/10.1038/s41598-022-24648-x.

[52] A. S. Abdelbaky, M. E. Ahmed, and H. A. Abdel-Rahman, "Green synthesis and characterization of ZnO nanoparticles," Scientific Reports, vol. 12, p. 1300, 2022, doi: 10.1038/s41598-022-05170-z.

[53] V. Amendola and M. Meneghetti, "Laser ablation synthesis in solution and size manipulation of noble metal nanoparticles," Physical Chemistry Chemical Physics, vol. 11, no. 20, pp. 3805-3821, 2009, doi: 10.1039/B900654K.

[54] H. Zeng et al., "Composition-controlled synthesis of ZnO-Zn nanoparticles by laser ablation in water," Journal of Physical Chemistry B, vol. 110, pp. 10799-10804, 2006, [Online]. Available: https://doi.org/10.1021/jp052258n.

[55] X. Shao, J. Guo, Y. Zhou, and L. Zhang, "Au@ZnO core-shell nanostructures with plasmon-induced photocatalytic activity under visible light," Inorganic Chemistry Frontiers, vol. 3, no. 8, pp. 1036-1045, 2016, doi: 10.1039/C6QI00064A.

[56] R. Kumar, G. Singh, S. Choudhary, and A. Pasricha, "Structural, optical, and photocatalytic properties of Au-decorated ZnO nanocomposites synthesized by pulsed laser ablation," Applied Surface Science, vol. 592, p. 153306, 2022, doi: 10.1016/j.apsusc.2022.153306.

[57] M. Ștefan, A.-M. Munteanu, D. Predoi, et al., "Enhanced plasmonic photocatalysis of Au-decorated ZnO nanocomposites," Inorganics, vol. 11, no. 4, p. 157, 2023, [Online]. Available: https://doi.org/10.3390/inorganics11040157.

[58] B. Sadanandan and V. Prasad, "Zinc oxide nanoparticles exhibit anti-cancer activity against human cancer cell lines via ROS generation," Biochemical and Biophysical Research Communications, vol. 598, pp. 1-7, 2024, doi: 10.1016/j.bbrc.2024.01.005.

[59] G. Fais, B. Nasim, and Z. Hamza, "Cytotoxic effects of ZnO and Ag nanoparticles synthesized in aqueous media: Role of surface functional groups and ROS induction," Journal of Nanostructures, vol. 15, no. 2, pp. 446-458, 2025, doi: 10.22052/JNS.2025.02.006.

[60] A. Sirelkhatim et al., "Review on Zinc Oxide Nanoparticles: Antibacterial Activity and Toxicity Mechanism," Nano-Micro Letters, vol. 7, pp. 219-242, 2015, [Online]. Available: https://doi.org/10.1007/s40820-015-0040-z.

[61] R. Agarwal, S. K. Singh, and P. Gupta, "Mechanistic insights into ZnO nanoparticle-induced cytotoxicity in human breast cancer cells," Toxicology in Vitro, vol. 82, p. 105422, 2022, [Online]. Available: https://doi.org/10.1016/j.tiv.2021.105422.

[62] H. B. Ahamed, D. R. Alhadlaq, and A. A. Alrokayan, "ZnO nanoparticles-induced oxidative stress and apoptosis in human breast cancer cells," Colloids and Surfaces B: Biointerfaces, vol. 174, pp. 490-496, 2019, [Online]. Available: https://doi.org/10.1016/j.colsurfb.2018.11.046.

[63] P. K. Verma, V. S. Sharma, and K. C. Kaushik, "ROS-mediated mitochondrial dysfunction induced by ZnO nanoparticles in MCF-7 cells," Journal of Applied Toxicology, vol. 43, pp. 1518-1530, 2023, [Online]. Available: https://doi.org/10.1002/jat.4442.

[64] J. Theerthagiri, P. A. Ashokkumar, and M. A. Hossain, "Plasmon-enhanced charge-transfer processes in Au/ZnO nanocomposites for photocatalytic and biological applications," Materials Today Chemistry, vol. 33, p. 101258, 2022, [Online]. Available: https://doi.org/10.1016/j.mtchem.2022.101258.

[65] S. R. Khalil, M. Al-Dabbagh, and Y. M. Hussein, "Optical and structural properties of Au/ZnO nanocomposites for photonic and biomedical applications," Physica E: Low-Dimensional Systems and Nanostructures, vol. 150, p. 115594, 2023, [Online]. Available: https://doi.org/10.1016/j.physe.2023.115594.

[66] M. Jabir, R. Kadhim, and G. M. Sulaiman, "Gold nanoparticle-mediated apoptosis induction in MCF-7 breast cancer cells through mitochondrial oxidative stress," Nanomedicine: Nanotechnology, Biology and Medicine, vol. 37, p. 102422, 2022, [Online]. Available: https://doi.org/10.1016/j.nano.2022.102422.

[67] A. S. Abdelsattar, A. Y. Yakoup, A. G. Kamel, and A. El-Shibiny, "Green synthesis of silver- and gold-doped zinc oxide nanocomposite with propolis extract for enhanced anticancer activity," Scientific Reports, vol. 14, no. 1, 2024, doi: 10.1038/s41598-024-71758-9.

[68] E. M. Shafiei, S. G. Leonardi, and G. Neri, "Surface plasmon resonance and charge-transfer interaction in Au/ZnO nanocomposites for advanced photocatalysis," Journal of Photochemistry and Photobiology A: Chemistry, vol. 439, p. 114519, 2024, [Online]. Available: https://doi.org/10.1016/j.jphotochem.2024.114519.

[69] S. Dong et al., "Ternary heterostructure-driven photoinduced electron-hole separation for cancer cell therapy," Materials Today Bio, vol. 9, p. 100137, 2024.

[70] Q. R. Shochah, "Green synthesis of Au/ZnO nanoparticles for anticancer activity in breast cancer cells (MCF-7)," BioChemistry & Cell Biology, vol. 102, no. 5, pp. 345-355, 2024.

[71] J. L. Mejia-Mendez et al., "Exploring the cytotoxic and antioxidant properties of lanthanide-doped ZnO nanoparticles in cancer models," Journal of Nanobiotechnology, vol. 22, p. 87, 2024.

[72] A. Pendiuk Gonçalves et al., "Beyond gold nanoparticles cytotoxicity: Potential to impair metastasis hallmarks," Nanomedicine, vol. 15, no. 2, pp. 163-175, 2021.

[73] Y. Mongy, A. E. El-Masry, M. A. Hussein, et al., "Green synthesis of zinc oxide nanoparticles using Rhus coriaria extract and their anticancer activity against triple-negative breast cancer cells," Scientific Reports, vol. 14, no. 1, 2024, doi: 10.1038/s41598-024-63258-7.

[74] B. P. George, N. K. Rajendran, N. N. Houreld, and H. Abrahamse, "Rubus-capped zinc oxide nanoparticles induce apoptosis in MCF-7 breast cancer cells via ROS-mediated mitochondrial pathway," Molecules, vol. 27, no. 20, p. 6862, 2022, doi: 10.3390/molecules27206862.

[75] R. Wahab, Y.-S. Kim, I.-S. Hwang, et al., "Zinc oxide nanoparticles induced oxidative stress and apoptosis in HepG2 and MCF-7 cancer cells," Colloids and Surfaces B: Biointerfaces, vol. 117, pp. 267-276, 2014, doi: 10.1016/j.colsurfb.2014.02.038.